# Recent Advancements in Outdoor Measurement Techniques for Angle of Incidence Effects

Bruce H. King[1], Daniel Riley[1], Charles D. Robinson[1] and Larry Pratt[2]

[1]Sandia National Laboratories, Albuquerque, NM, 87185-0951, USA
[2]CFV Solar Test Lab, Albuquerque, NM, 87110, USA

***Abstract* — Reflection losses from a PV module become increasingly pronounced at solar incident angles >60°. However, accurate measurement in this region can be problematic due to tracker articulation limits and irradiance reference device calibration. We present the results of a measurement method enabling modules to be tested over the full range of 0-90° by articulating the tracker in elevation only. This facilitates the use of a shaded pyranometer to make a direct measurement of the diffuse component, reducing measurement uncertainty. We further present the results of a real-time intercomparison performed by two independent test facilities ~10 km apart.**

***Index Terms* — angle of incidence, diffuse irradiance, incident angle modifier, outdoor testing, PV modules, pyranometer calibration.**

## I. Introduction

The majority of flat plate PV modules are mounted in a fixed orientation such that the incident irradiance is rarely directly normal to the surface of the module. Two energy loss mechanisms arise due to the Angle of Incidence (AOI) effects on direct normal irradiance (DNI). The first, cosine loss due to the projection of the direct irradiance onto the tilted module surface, is easily accounted for given sun position and module orientation. The second, reflection of the direct incident irradiance, becomes more pronounced at incidence angles greater than ~ 50°, and is affected by the optical properties of the module. Accurate performance models for PV system energy prediction rely on being able to effectively represent the reflective loss component due to angle of incidence.

King [1] presented a method for experimentally measuring the AOI response of a module outdoors using a two-axis tracker to articulate the module to achieve a range of AOI. More recent work [2] has built upon and validated this basic methodology. A key outcome of the more recent study is the recommendation that AOI need not be measured for standard flat plate modules with uncoated glass [3].

Factors such as texture, anti-reflective coatings, soiling, glass composition or the use of a polymeric cover, may change the scattering and reflective properties of the glass-air interface and the AOI response of a PV module. In these cases, use of the "standard" loss function [2 - 4] is not appropriate. As module manufacturers explore options to enhance the efficiency of their products or achieve a level of differentiation from commodity products, there continues to be a need to characterize the AOI response of modules. Testing is often limited to certain times of day or certain times of year due to tracker articulation limits. Knisley et al [2] were restricted to testing around 2:30pm and noted articulation limits that made characterization above ~65° AOI challenging. As noted by Fanney [5], the region > 65° is precisely where AOI effects become pronounced. Another challenge noted in earlier studies is the impact that pyranometer calibration has on the results. It has been shown [6, 7] that pyranometers do not exhibit perfect cosine response to solar AOI and variation can exceed 10%. Global plane of array (POA) pyranometers used for AOI characterization must therefore be appropriately calibrated to obtain accurate results.

Here, we present a novel method of measuring the AOI response of a module. Using a customized tracker with extended travel, the module can be articulated through the full range of 0-90° AOI by rotating only the elevation axis while the azimuthal axis continues to track the sun. This enables the use of a simple method to use measured diffuse irradiance rather than calculated diffuse irradiance (global POA minus cosine adjusted DNI) during analysis. This has several advantages. First, the uncertainty of the POA diffuse measurement is smaller than the uncertainty in a calculated POA diffuse. Second, calculating global POA from measured diffuse POA and direct normal irradiance (DNI) removes the need for an AOI correction for a global POA pyranometer.

Fig. 1. Diffuse POA irradiance measurement for elevation-only rotations

We also present the results of a real-time round robin conducted between Sandia and CFV Solar comparing the AOI measurements made simultaneously with different trackers, utilizing different control methods under essentially the same sky conditions. To our knowledge, this is the first time such an intercomparison has been attempted.

## II. Derivation of $f_2(\theta)$

To our knowledge, the derivation of the $f_2(\theta)$ function found in the Sandia Array Performance Model has never been published in full [1-5]. Since the new method of accounting for diffuse irradiance relies on a modification of this derivation, we present it here for completeness.

TABLE I
SUMMARY OF NOMENCLATURE

| | |
|---|---|
| $E_e$ | Effective solar irradiance that reaches the cells (dimensionless) |
| $E_o$ | Reference irradiance (1000 W/m$^2$) |
| $E_b$ | Beam component of irradiance (W/m$^2$) |
| $E_{DNI}$ | Direct normal irradiance (W/m$^2$) |
| $E_{diff}$ | Global diffuse irradiance (W/m$^2$) |
| $E_{POA}$ | Global irradiance on the plane of the module (W/m$^2$) |
| $f_1(AM)$ | Empirical function relating air mass to $I_{sc}$ as a proxy for solar spectral influence (dimensionless) |
| $f_2(\theta)$ | Empirical function relating reflection losses due to solar incidence angle to $I_{sc}$ (dimensionless) |
| $I_{sc}$ | Short circuit current (A) |
| $I_{sco}$ | Short circuit current at STC (A) |
| $I_{scr}$ | Reference short circuit current measured at 0° incidence angle during determination of $f(\theta)$(A) |
| $T_c$ | Cell temperature inside module (°C) |
| $T_m$ | Module back sheet temperature (°C) |
| $T_0$ | Reference temperature (25°C) |
| $\Delta T$ | Reference temperature difference between module back sheet and cell (3°C) |
| $f_d$ | Fraction of diffuse irradiance used by the module (dimensionless) |
| $\alpha_{Isc}$ | Short circuit current temperature coefficient (1/°C) |
| $\theta$ | Incident angle between the direct beam and the normal to the module surface (°), AOI |

### *A). General form of $f_2(\theta)$*

The Sandia Photovoltaic Array Performance Model (SAPM) relationship for short circuit current is given by

$$I_{sc} = I_{sco} E_e \left[1 + \alpha_{Isc}[T_c - T_0]\right] \quad (1)$$

The effective irradiance, $E_e$, accounts for spectral changes due to airmass variation, cosine and reflective losses from the front surface of the module, and capture of diffuse light.

$$E_e = f_1(AM) \frac{E_b f_2(\theta) + f_d E_{diff}}{E_0} \quad (2)$$

The term, $f_d$, is included in (2) to account for modules that do not utilize 100% of the incident diffuse light. It is assumed in (2) that only the direct beam component is reflected at high angles of incidence and that the diffuse component is absorbed according to $f_d$, regardless of its incident angle. The beam component of irradiance, $E_b$, is related to the measured DNI ($E_{DNI}$) simply by

$$E_b = E_{DNI} \cos\theta \quad (3)$$

Combining (1), (2) and (3) results in Eqn (1) found in [4].

$$I_{sc} = I_{sco} f_1(AM) \left[\frac{E_b f_2(\theta) + f_d E_{diff}}{E_0}\right] \left[1 + \alpha_{Isc}[T_c - T_0]\right] \quad (4)$$

In the SAPM, $I_{sco}$ represents the short circuit current at STC conditions. However, for this analysis, it is preferred to use a local reference value, determined at the time of the measurement. Defining the reference value $I_{scr}$ and recognizing that by definition $f_2(\theta=0)=1$, Equation (4) may be rearranged to yield

$$I_{scr} = \frac{I_{sc} E_0}{f_1(AM)\left[E_b + f_d E_{diff}\right]\left[1 + \alpha_{Isc}[T_c - T_0]\right]} \quad (5)$$

The experimental determination of $I_{scr}$ will be discussed in more detail below in Section IV. The $f_2(\theta)$ function may then be found by rearranging (4),

$$f_2(\theta) = \frac{\left[\frac{I_{sc}}{I_{scr}}\right]\left[\frac{E_0}{f_1(AM)\left[1 + \alpha_{Isc}[T_c - T_0]\right]}\right] - f_d E_{diff}}{E_b} \quad (6)$$

In practice, further simplifications are typically used. It is important to note that in the more general forms of (5) and (6) that the airmass and diffuse utilization factors are retained. If (5) is substituted into (6), it can be shown that $f_2(\theta)$ depends on the ratio of the airmass at the time the reference condition is established to the airmass at any other time during the test. Provided that the test is conducted over a short enough time period, changes in airmass can be ignored and this term cancels out. However, if the test is conducted across a long enough period of time or during a time of day when airmass is changing rapidly, this simplification may no longer hold and a correction for airmass differences is required.

### *(B). Application to Specific Test Methods*

As shown in (6) $f_2(\theta)$ depends on two components of the incident irradiance; the direct beam component, $E_{DNI}$ and the diffuse component, $E_{diff}$. Together, these make up the global plane of array, $E_{POA}$. The three quantities are related through

$$E_{POA} = E_b + E_{diff} \quad (7)$$

While all three of these parameters can be measured independently, in practice most typical irradiance instruments are not calibrated accurately enough for calculated and measured values to be interchangeable. Therefore, it is recommended to measure two of the above quantities and calculate the third, even in cases where all three measurements may be available. The choice of which two to measure will be determined by the available instrumentation and capabilities of the tracker. It is important to maintain consistency throughout the analysis; if the calculated value of $E_{POA}$ is used in one part of the analysis, then it should be used in all parts of the analysis.

In each of the following cases, it is assumed that $f_1(AM)$ = constant and $f_d = 1$.

*i). Measured global POA and DNI (standard method):* In the standard method, $E_{DNI}$ is measured using a pyrheliometer mounted on an independent weather tracker, $E_{POA}$ is measured using a global pyranometer mounted in the test plane and $E_{diff}$

is calculated by rearranging Equation (7). The reference $I_{scr}$ and $f_2(\theta)$ functions are given by

$$I_{scr} = \frac{I_{sc}E_0}{E_{POA}\left[1 + \alpha_{Isc}[T_c - T_0]\right]} \quad (8)$$

and

$$f_2(\theta) = \frac{\left[\frac{I_{sc}}{I_{scr}}\right]\left[\frac{E_0}{1 + \alpha_{Isc}[T_c - T_0]}\right] - E_{POA} + E_{DNI}\cos\theta}{E_{DNI}\cos\theta} \quad (9)$$

This is the standard method first described in [1] and captured in IEC61853-2 [3]. However, this method has the potential to introduce inaccuracy due to the requirement for a global pyranometer that has been calibrated for angle-of-incidence response, particularly at high incidence angles [2]. Particular attention should be paid to this calibration if high accuracy AOI measurement is desired.

*ii). Measured diffuse POA and DNI (new method)*: In the new method, $E_{DNI}$ is measured using a pyrheliometer mounted on an independent weather tracker, $E_{diff}$ is measured using a diffuse pyranometer mounted in the test plane (more detail in Section III) and $E_{POA}$ is calculated by rearranging Equation (7). The reference $I_{scr}$ and $f_2(\theta)$ functions are given by

$$I_{scr} = \frac{I_{sc}E_0}{\left[E_{DNI} + E_{diff}\right]\left[1 + \alpha_{Isc}[T_c - T_0]\right]} \quad (10)$$

and

$$f_2(\theta) = \frac{\left[\frac{I_{sc}}{I_{scr}}\right]\left[\frac{E_0}{1 + \alpha_{Isc}[T_c - T_0]}\right] - E_{diff}}{E_{DNI}\cos\theta} \quad (11)$$

This new method was enabled by the development of a test tracker and control system that enables pure elevation articulation to high incidence angles. While this type of test platform is not typical, it enables the use of a measured diffuse value, removing the need to have an AOI corrected pyranometer.

*iii). Measured global and diffuse POA (simplified method)*: In this method, both $E_{POA}$ and $E_{diff}$ are measured using pyranometers mounted in the test plane, while $E_{DNI}$ is calculated. The reference $I_{scr}$ and $f_2(\theta)$ functions are given by,

$$I_{scr} = \frac{I_{sc}E_0}{E_{POA}\left[1 + \alpha_{Isc}[T_c - T_0]\right]} \quad (12)$$

and

$$f_2(\theta) = \frac{\left[\frac{I_{sc}}{I_{scr}}\right]\left[\frac{E_0}{1 + \alpha_{Isc}[T_c - T_0]}\right] - E_{diff}}{E_{POA} - E_{diff}} \quad (13)$$

This method offers a simplification in that both the global and diffuse POA instruments are mounted in the test plane with the module under test, eliminating the need for DNI measurements to be made on a second tracker. However, it is anticipated that this method will be less accurate than either of the other two methods because it eliminates the use of the pyrheliometer, which is generally a more accurate instrument than the pyranometers. The validity of this method was not investigated as part of the study, but it is presented here for completeness.

## III. Experimental Procedure

The measurement procedures largely follow the methodology described by [5] and are consistent with IEC 61853-2.

### *A. Equipment*

The following equipment was used for conducting these tests;

- Three Azimuth-Elevation solar trackers capable of rotating the PV module over an AOI range between 0° and 90°, designated SNL1, SNL2 and CFV.
- AOI-corrected pyranometers measuring global POA irradiance ($E_{POA}$), mounted in the module test plane
- Pyranometer measuring the diffuse POA irradiance ($E_{diff}$), mounted in the module test plane (SNL2 only)
- Pyrheliometers measuring DNI ($E_{DNI}$), mounted on separate weather trackers
- Means of measuring $I_{sc}$ of the PV module under test
- Means of measuring the average temperature of the PV module under test.
- Four nominally identical PV modules (SunTech STP085S-12Bb-1)

All of the trackers are located in Albuquerque, NM. Trackers SNL1 and SNL2 are approximately 25 m apart, and 10 km from the CFV tracker. The SNL2 tracker has the ability to rotate a full 180° in elevation, while the SNL1 and the CFV trackers do not.

### *B. Test Objectives and Methods*

The objectives of this study were to;

- Compare the consistency between trackers when performing three different types of tracker articulation
- Demonstrate the use of elevation only/measured diffuse for performing an AOI characterization
- Perform a real-time intercomparison between Sandia and CFV under nominally identical sky conditions
- Perform an assessment of seasonal variations in AOI measurements.

Three types of articulation methods were compared. For the first articulation method, referred to as "tracker elevation = 10°," the elevation axis was rotated down to an elevation of 10° above the horizon while the azimuthal axis continued to track the Sun. This elevation was then held constant while the azimuthal axis was rotated to achieve the desired AOI. For the second articulation method, referred to as "sun elevation + 7°," the elevation axis was rotated up to point 7° above the

current sun elevation while the azimuthal axis continued to track the Sun. The relative elevation offset above the Sun was then maintained while the azimuthal axis was rotated to achieve the desired AOI. For the final tracker articulation method, referred to as "elevation only," the elevation axis was rotated over the full range of 0°-90° relative to the Sun while the azimuthal axis continued to track the Sun. All three trackers were capable of performing the first two methods while only the SNL2 tracker was capable of performing the "elevation only" method. There are benefits and drawbacks to each of these methods, discussed below in Section V.

The first two sets of tests were performed exclusively at Sandia. First, the four PV modules were characterized simultaneously (two on each tracker) using the "tracker elevation = 10°" rotation method to evaluate the consistency between trackers. Two of the modules were then interchanged and the test repeated on the same day. Next, the four PV modules were characterized simultaneously using the "tracker elevation = 10°" and "elevation only" rotation methods on SNL1 and SNL2, respectively. Again, two modules were interchanged and the test repeated on the same day.

Two of these modules were then transferred to CFV. Sandia and CFV then performed simultaneous testing where CFV used the "tracker elevation = 10°" rotation method, while Sandia performed the "tracker elevation = 10°" rotation method on SNL1 and "elevation-only rotation" method on SNL2. On the next day of testing, CFV and SNL1 simultaneously used the "sun elevation + 7°" method while SNL2 operated in the elevation-only mode.

Sandia then conducted a final set of tests close to the vernal equinox, in which the two PV modules at Sandia were again characterized simultaneously using the "tracker elevation = 10°" and "elevation only" rotation methods on SNL1 and SNL2, respectively. Unfortunately, the signal from the diffuse pyranometer on SNL2 was lost during the equinox test, so only results from the SNL1 tracker are reported here.

## IV. Analysis

The measured IV summary data ($I_{sc}$), module backsheet temperatures ($T_m$), irradiance measurements ($E_{POA}$, $E_{DNI}$, $E_{diff}$), sun azimuth and elevation and tracker plane of array position data were merged into a single time synchronized data set. Points collected while the tracker was in motion between target incidence angles ($\theta$) were removed. Angle of incidence was calculated for each data point from the known sun position and the tracker position using Eqn (1) in reference [1]. The temperature coefficient ($\alpha_{Isc}$) for one module was determined outdoors under natural sunlight using a local Sandia test procedure based on [8] and applied to all four all modules under test. Cell temperatures were calculated from module temperatures according to [4].

$$T_c = T_m + \frac{E_{POA}}{E_0}\,\Delta T \qquad (14)$$

It is important to note that the value of $E_{POA}$ used for each calculation was determined according to (7) and was consistent with the specific test method.

From the assembled data set, a minimum of 5 measurements made at ($\theta = 0$), just before the module was taken off sun, were identified. The average of these values was then used to determine $I_{scr}$ using either (8) or (10), depending on the method under evaluation. Finally, $f_2(\theta)$ was calculated using either (9) or (11).

## V. Results and Discussion

### A. Differences Between Modules on Different Trackers

The results testing using the "tracker elevation = 10°" method are shown in Fig. 2. These measurements revealed that modules of the same make and model exhibit similar AOI characteristics, in line with expectations [2, 3]. For clarity, only the modules that were swapped between trackers are shown in Fig. 2.

These tests also revealed a difference between loss factors determined on the two trackers. Loss factors determined on the SNL1 tracker were consistently lower than those determined on the SNL2 tracker. The difference was predominantly seen at high incidence angles. We believe that this difference is likely due to uncertainty in the AOI calibration of the global POA pyranometers used on each tracker.

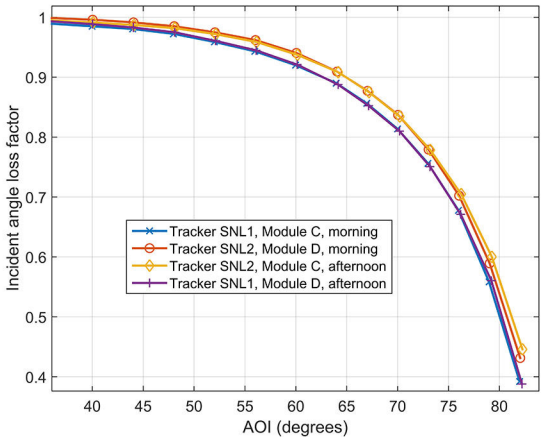


Fig. 2. Modules C and D, tested simultaneously using the "10° elevation" rotation method, then swapped between trackers

### B. Differences Between Tracker Articulation Methods

Fig. 3 shows the results of tests using the three different tracker articulation methods. For clarity, results are shown for only a single module. The "tracker elevation = 10°" and "elevation only" rotation methods were performed on SNL2 while "sun elevation + 7°" was performed on the CFV tracker. From this plot, it can be seen that the method of tracker articulation can play a significant role in the determination of the incident angle loss factor. Notably, the curve obtained using "tracker elevation = 10°" produced a much lower curve

than the other articulation methods at AOI greater than 50°. Further, measurement using the "elevation only" method and calculated (rather than measured) diffuse causes the incident angle loss factor to rise slightly above unity at intermediate AOI. Since this is theoretically impossible, we conclude the error is associated with measurement of the global POA (discussed further below).

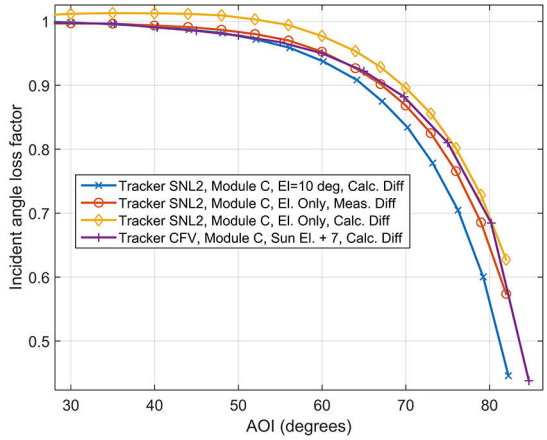


Fig. 3. Module C tested using the "10° elevation" rotation method, the "elevation only" method (calculated and measured diffuse irradiance), and the "Sun elevation + 7°" rotation method

For the "tracker elevation = 10°" method, the relative amount of sky and ground "viewed" by the PV module changes early in the test, with the amount of ground reflected irradiance increasing. This appears to be a drawback. This method is also susceptible to specular reflections from objects on the ground such as car windshields, buildings, water, etc. However, the method can be achieved by most commercial two axis trackers and can achieve a large range of AOI when the sun has a high elevation angle.

The "sun elevation + 7°" method provides the most consistent ratio of sky and ground viewed by the module, and can also be achieved by most two axis trackers. However, when the sun is at a high elevation angle, this method is unable to achieve a large range of AOI. Thus, a characterization test may need to be conducted either in the morning or afternoon, when solar conditions (e.g. air mass) may be changing more rapidly, which generally reduces the flexibility of the test.

For the "elevation only" method, the relative amount of sky and ground viewed by the PV module changes throughout the test. Initially, the amount of sky viewed increases until the tracker is pointed at the zenith and then decreases as the test progresses. However, the "elevation only" method allows for a relatively simple method to measure the diffuse irradiance in the plane of the array. This method also simplifies movement to a desired AOI; in contrast, moving to a desired AOI with a combination elevation and azimuth moves requires significantly more calculation. This method cannot be performed by many commercial two axis trackers, which have articulation limits on the elevation axis that only allow them to point toward the zenith.

### *C. Measured Diffuse POA Irradiance*

Test results evaluating the "elevation only" method are shown in Figure 4. Due to articulation limits of the other two trackers, this test was only performed on the SNL2 tracker. Here, the measured diffuse irradiance (Fig. 1) is used for all analysis rather than calculated diffuse. As shown in Fig. 3, calculating the diffuse irradiance from a test performed only in elevation causes a rise in the calculated loss factor to above unity. This rise in loss factor (normalized $I_{SC}$) is completely mitigated when the measured diffuse irradiance is used. Tests conducted across multiple days and multiple modules revealed that use of the measured diffuse irradiance for the analysis produces extremely consistent response curves as shown in Fig. 4.

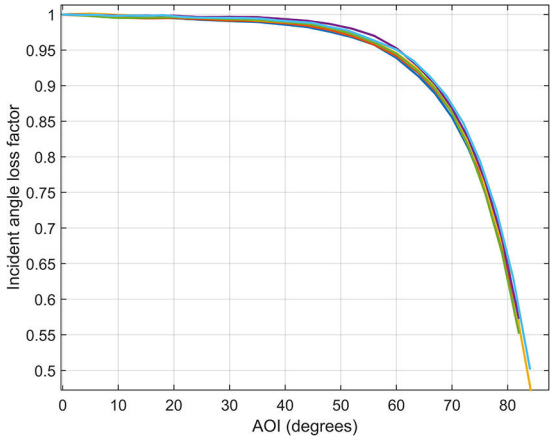


Fig. 4. Six tests over four different modules using "elevation only" articulation and measured diffuse irradiance; maximum deviation between tests is approximately 1%

### *D. Comparing Results from SNL and CFV*

Through similar tests conducted simultaneously at Sandia and CFV, we have determined that test processes to determine AOI loss factors are repeatable across labs, and provide similar results under similar environmental conditions. As shown in Fig. 5, tests between the SNL2 tracker and the CFV tracker generate very similar response curves, despite the difference in location, hardware and articulation method. The tests on the SNL1 tracker consistently provide a lower response, which we believe is due to the difference in the incident angle calibration for the pyranometers.

### *E. Seasonal Effects of AOI Testing*

Sandia's testing of the same module, using the same test procedures, near the winter solstice and the vernal equinox show that seasonal changes appear to have little influence on the test data generated for incident angle characterization.

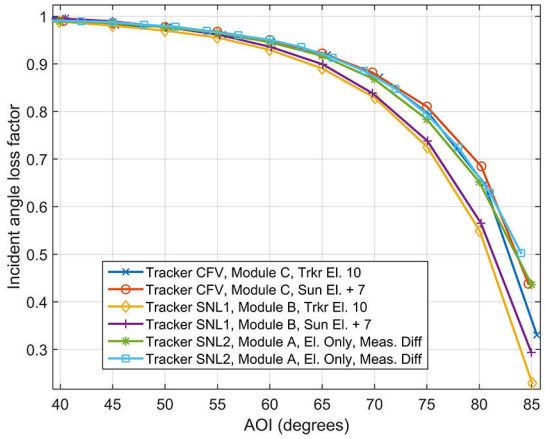


Fig. 5. Incident angle loss factors determined from 6 tests with varying location, reference device and rotation method. Legend entries 1, 3, and 5 were conducted simultaneously, while 2, 4, and 6 were conducted simultaneously.

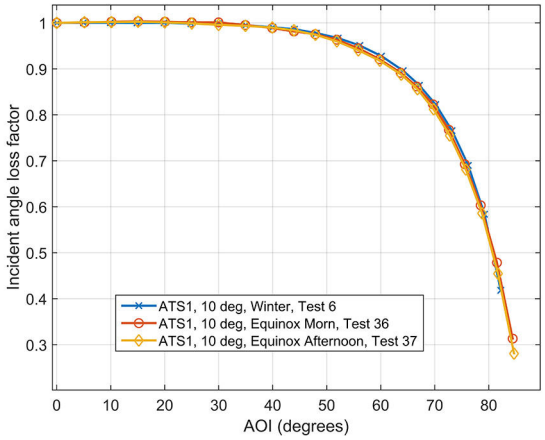


Fig. 6. Incident angle loss factors for the same module tested at different times of year

## V. Conclusions

We have demonstrated two improvements in the angle of incidence characterization of flat plate PV modules. First, articulation of the tracker over the full range of 0-90° in elevation only allows accurate positioning and measurement to be made near solar noon when sky conditions are changing the least. Second, this articulation method facilitates the use of a shaded pyranometer to directly measure the diffuse component. Measured diffuse eliminates uncertainty introduced by subtracting AOI adjusted DNI from measured global POA and avoids the need for an AOI correction for the pyranometer.

However, few test labs have access to such specialized tracking capabilities. By performing a real-time intercomparison between two independent test labs located approximately 10km apart, we have demonstrated tracker articulation methods that provide acceptable results when tracker travel is limited.

From these observations, we feel that we can recommend several practices which should be considered when developing an AOI characterization plan for PV modules.

If possible, measuring the diffuse POA irradiance incoming to the module and subsequently calculating the global POA irradiance generates the best possible data. This also removes the necessity to calibrate a global POA irradiance-measuring pyranometer for AOI, and can reduce the uncertainty in the resulting performance curves caused by uncertainty in the pyranometer AOI calibration.

If it is not possible to measure the diffuse POA irradiance, it is preferable to measure the global POA irradiance using a pyranometer that has only a small (or no) required correction for incident angle. Additionally, a tracker articulation method which provides the PV module with a consistent "view" of the ratio of sky and ground provides more consistent results if diffuse POA cannot be measured.

## Acknowledgements

This work was supported by the U.S. Department of Energy SunShot Initiative. Sandia National Laboratories is a multi-program laboratory managed and operated by Sandia Corporation, a wholly owned subsidiary of Lockheed Martin Corporation, for the U.S. Department of Energy's National Nuclear Security Administration under contract DE-AC04-94AL85000.

## References

[1] D. L. King, J. A. Kratochvil and W. E. Boyson, "Measuring Solar Spectral and Angle-of-Incidence Effects on Photovoltaic Modules and Solar Irradiance Sensors," in *26th IEEE Photovoltaic Specialists Conference,* 1997, p. 1113.

[2] B. Knisley, S. V. Janakeeraman, J. Kuitche, G. TamizhMani, "Validation of Draft International Electrotechnical Commission 61853-2 Standard: Angle of Incidence Effect on Photovoltaic Modules," Solar America Board for Codes and Standards, 2013.

[3] Future IEC 61853-2 Ed. 1.0

[4] D. L King, W. E. Boyson, and J. A. Kratochvil, "Photovoltaic Array Performance Model," Sandia National Laboratories, SAND2004-3535, (2004).

[5] A. H. Fanney, M. W. Davis, B. P. Dougherty, D. L. King, W. E. Boyson, J. A. Kratochvil, "Comparison of Photovoltaic Module Performance Measurements," *Transactions of the ASME*, Vol. 128, May 2006, p. 152.

[6] D. L King and D. R. Myers, "Silicon-Photodiode Pyranometers: Operational Characteristics, Historical Experience, and New Calibration Procedures," in *26th IEEE Photovoltaic Specialists Conference,* 1997.

[7] J. J. Michalsky, L. C. Harrison, W. E. Berkheiser, "Cosine response characteristics of some radiometric and photometric sensors," *Solar Energy*, Vol 54 (6), 1995, p. 397.

[8] D. L. King, J. A. Kratochvil, and W. E. Boyson, "Temperature Coefficients for PV Modules and Arrays: Measurement Methods, Difficulties and Results," in *26th IEEE Photovoltaic Specialists Conference,* 1997, p. 1183.